

ELECTRON TRAJECTORIES IN A COMBINED WIGGLER AND ALTERNATING GRADIENT QUADRUPOLE FIELD\*

T. F. Wang and R. K. Cooper, AT-6, MS H829  
Los Alamos National Laboratory, Los Alamos, NM 87545

Summary

This paper reports on studies of electron trajectories in a combined wiggler and alternating gradient quadrupole field. The quadrupole field is assumed to vary continuously along the symmetry axis. The linearized equations of electron motion are solved analytically for a plane-polarized wiggler by using the two-scale perturbation method. A comparison with the numerical solution is presented, and the conditions for unstable trajectories are discussed.

Introduction

Recently, there has been a growing interest in the study of using free-electron lasers (FELs) to generate coherent and tunable XUV radiation at high intensity.<sup>1</sup> It has been pointed out<sup>2</sup> that to achieve an equal gain in the UV or XUV regime, an FEL needs much higher density in the electron beam and longer wiggler length than an FEL operated in the infrared or visible-light region. Thought is then directed toward using an external focusing channel along with the wiggler in the XUV FEL design.

In this paper, we shall study electron trajectories in combined wiggler and quadrupole fields. Our study will be limited to the plane-polarized wigglers for FELs to be operated in the UV or XUV ranges only. The quadrupole channel considered here is one in which the field quadrupole gradient varies alternately and continuously along the symmetry axis. The wiggler's field is assumed to be concentric with that of the quadrupole channel. To make the analysis tractable, the self-field of the electron beam is ignored, the nonlinear components of the wiggler field are neglected, and the axial speed of electrons is assumed to be constant.

Because of the lengthy and tedious calculations, the details of solving the trajectory equations will not be included here. Interested readers can find details in internal reports by authors.<sup>3,4</sup>

Equations of Motion

We choose a Cartesian coordinate system so that the electrons are traveling in the z-direction and the wiggler field is in the y-direction. The z-axis is assumed to coincide with the symmetry axis of the concentric wiggler and quadrupole fields. The origin of the coordinate system is chosen at the entrance of the wiggler/quadrupole channel. We also assume that the wiggler/quadrupole channel extends over all  $z \geq 0$ . The variation of the wiggler field along the z-direction can be written as  $B_w \cos(2\pi z/\lambda_w)$ , where  $B_w$  is the amplitude of the wiggler magnetic field,  $\lambda_w$  is the wavelength of the wiggler, and we have neglected the fringe field at the entrance. The quadrupole field considered here can be represented as  $-B' \sin(2\pi z/\lambda_Q)$  and  $B' \sin(2\pi z/\lambda_Q)$ , in the x- and y-directions, respectively, where  $B'$  is the field gradient and  $\lambda_Q$  is the quadrupole period.

Neglecting the self-field of the beam and assuming the laser field is absent, the equations of motion for an electron are

$$m \frac{d}{dt} (\gamma \frac{dx}{dt}) = qB_w \sinh(k_w y) \sin(k_w z) \frac{dy}{dt} \tag{1}$$

$$- qv_z B' x \sin(k_Q z) + qv_z B_w \cosh(k_w y) \cos(k_w z) ,$$

and

$$m \frac{d}{dt} (\gamma \frac{dy}{dt}) = -qB_w \sinh(k_w y) \sin(k_w z) \frac{dx}{dt} \tag{2}$$

$$+ qv_z B' y \sin(k_Q z) ,$$

where  $m$  is the mass of an electron,  $\gamma$  is the ratio of an electron's total energy to the quantity  $mc^2$  ( $c$  = the speed of light),  $t$  is the time,  $q$  is the unit charge,  $k_w = 2\pi/\lambda_w$ ,  $k_Q = 2\pi/\lambda_Q$  and  $v_z$  is the axial speed of the electron. Neglecting  $dy/dt$  in Eq. (1) and using the approximations of  $\sinh(k_w y) \approx k_w y$ ,  $\cosh(k_w y) \approx 1$ ,  $v_z \approx c$ , and  $ct \approx v_z t = z$ , one obtains from Eqs. (1) and (2) that

$$\frac{d^2 x}{dz^2} = k_w [a_w \cos(k_w z) - k_w x b \sin(Kk_w z)] , \text{ and } \tag{3}$$

$$\frac{d^2 y}{dz^2} = k_w^2 [-a_w \sin(k_w z) (\frac{dx}{dz}) + b \sin(Kk_w z)] y , \tag{4}$$

where  $K = k_Q/k_w$ ,  $a_w = qB_w/m\gamma ck_w$ , and  $b = qB'/m\gamma ck_w^2$ .

Solutions for  $K \ll 1$ ,  $a_w \ll K^{3/2}$ , and  $b \ll K^2$

In this range, good approximations of the solutions to Eqs. (3) and (4) can be found by using the two-scale perturbation method.<sup>4</sup> Retaining the first few lower order terms in the perturbation series, we have

$$x(z) = C e^{U_x(z)} \sin[\phi + V_x(z)] \tag{5}$$

$$+ \left(\frac{a_w}{k_w \sin \psi}\right) e^{U_x(z)} \sin[\psi - V_x(z)] + W(z) ,$$

$$\text{and } y(z) = D e^{U_y(z)} \sin[\theta + V_y(z)] , \tag{6}$$

where  $C$ ,  $\phi$ ,  $D$ , and  $\theta$  are constants dependent on the initial conditions

$$U_x(z) = \left[\frac{b}{K^2}\right] \sin(k_Q z) + \left(\frac{-b}{8K^2}\right) \cos(2k_Q z) + \dots , \tag{7}$$

$$V_x(z) = \frac{1}{\sqrt{2}} \left(\frac{b}{K^2}\right) k_Q z + \sqrt{2} \left(\frac{b}{K^2}\right)^2 \cos(k_Q z) + \dots , \tag{8}$$

\*Work supported by the US Dept. of Defense and the Ballistic Missile Defense Advanced Technology Center.

$$U_y(z) = -\frac{a_w^2}{8} \cos(2k_w z) - \frac{b}{K^2} \left(1 + \frac{2a_w^2}{K^2} + \frac{7b^2}{4K^4}\right) \sin(k_Q z) + \frac{b^3}{36K^6} \sin(3k_Q z) + \frac{b^2}{8K^4} \cos(2k_Q z) + \dots, \quad (9)$$

$$V_y(z) = \sqrt{\frac{1}{2} \left(a_w^2 + \frac{b^2}{K^2}\right)} \left\{ \left[ 1 + \left( \frac{b^2}{a_w^2 K^2} + b^2 \right) \left( \frac{a_w^2}{K^2} + \frac{25b^2}{32K^4} \right) \right] k_w z - \frac{5b^2}{8K^5} \sin(2k_Q z) - \frac{2b}{K^3} \cos(k_Q z) \right\} + \dots, \quad (10)$$

$$W(z) = \frac{a_w b}{2k_w} \left[ \frac{\sin(k_w - k_Q)z}{(1-K)^2} - \frac{\sin(k_w + k_Q)z}{(1+K)^2} \right] - \left( \frac{a_w}{k_w} \right) \cos(k_w z) + \dots, \quad (11)$$

$$\text{and } \psi = \tan^{-1} \left( \frac{1-K^2}{\sqrt{2}} \right) + \dots. \quad (12)$$

In Eq. (5), the general solution of x-motion is contained in the first term and the particular solution is written into the second and third terms. The first and second terms describe the betatron oscillations induced by the quadrupole and the wiggler, respectively. The third term describes the fast oscillation excited by the wiggler. Note that the particular solution is independent of  $C$  and  $\phi$ ; therefore, the oscillations induced by the wiggler should be coherent motions for all electrons in the beam as we expected. Also, because the second term in Eq. (5) has the same form as the general solution, the quantity  $W(z)$  must satisfy Eq. (3).

The quantities  $U_x(z)$  and  $V_x(z)$  in the x-solution are related to each other by

$$\frac{dV_x}{dz} = \frac{bk_w}{K\sqrt{2}} e^{-2U_x(z)} \left[ 1 - \frac{7}{32} \left( \frac{b}{K^2} \right)^2 + \dots \right], \quad \text{and} \quad (13)$$

$$\frac{d^2 U_x}{dz^2} + \left( \frac{dU_x}{dz} \right)^2 = \left( \frac{dV_x}{dz} \right)^2 - bk_w^2 \sin(k_Q z). \quad (14)$$

For the y-solution, one can derive similar relations between  $U_y(z)$  and  $V_y(z)$ . These relations will be helpful when we study the beam envelopes and matching.

#### Stable Solutions for $K \ll 1$ , $a_w \sim K$ , and $b \ll K^2$

If we lower the electron energy and/or increase the quadrupole period, we then may reach the range of  $K \ll 1$ ,  $a_w \sim K$ , and  $b \ll K^2$  where the unstable solution is likely to occur. Like Mathieu's equation, there are boundaries between the stable and unstable zones. In fact, for  $K \ll 1$ , the stability boundaries of the Mathieu's equation,

$$\frac{d^2 y}{dz^2} + k_w^2 \left[ \frac{a_w^2}{2} - b \sin(Kk_w z) \right] y = 0, \quad (15)$$

can be very good approximations to those of Eq. (4). More accurate boundaries can be calculated by using a

perturbation method. It can be shown that the first two stable zones for Eq. (4) are<sup>3</sup>

$$-\frac{b^2}{K^4} + \frac{14b^4}{27K^8} + \dots < \frac{a_w^2}{K^2} < \frac{1}{2} - \frac{b}{K^2} - \frac{b^2}{4K^4} - \frac{K^2}{64} + \dots, \quad \text{and} \quad (16)$$

$$\frac{1}{2} + \frac{b}{K^2} - \frac{b^2}{4K^4} - \frac{K^2}{64} + \dots < \frac{a_w^2}{K^2} < 1 - \frac{b^2}{6K^4} - \frac{K^2}{4} + \dots.$$

Stable solutions for parameter values far from the stability boundaries also have been derived from the two-scale perturbation method. The x-solution in this region is identical to that in the last section, and the y-solution has the same form as in Eq. (6) except that the expressions of  $U_y(z)$  and  $V_y(z)$  are different from Eqs. (9) and (10). The approximations to  $U_y(z)$  and  $V_y(z)$  are

$$U_y(z) \approx \frac{b \sin(k_Q z)}{(2a_w^2 - K^2)} - \frac{a_w^2}{8} \cos(2k_w z) - \frac{b^2(4a_w^2 + K^2) \cos(2k_Q z)}{4(2a_w^2 - K^2)^2 (a_w^2 - 2K^2)} + \dots, \quad (17)$$

and

$$V_y(z) \approx \frac{a_w}{\sqrt{2}} \left\{ \left[ 1 + \frac{a_w^2}{32} - \frac{b^2}{2a_w^2(2a_w^2 - K^2)} \right] k_w z + \frac{a_w^2}{8} \sin(2k_w z) + \frac{2b \cos(k_Q z)}{K(2a_w^2 - K^2)} + \frac{b^2(2a_w^2 + 5K^2) \sin(2k_Q z)}{4K(2a_w^2 - K^2)^2 (a_w^2 - 2K^2)} \right\} + \dots. \quad (18)$$

Relations similar to Eqs. (13) and (14) can be derived also.

#### Numerical Examples and Comparison with Numerical Solutions

We now present some of our numerical results and compare the analytical solutions with the numerical solutions of Eqs. (3) and (4) by the Runge-Kutta method. For the examples given below, because of the excellent agreement there is almost no discernible difference between the plots for these two kinds of computational results. We therefore shall use one figure to show both the numerical and the analytical solutions.

In the range of  $K \ll 1$ ,  $a_w \ll K^{3/2}$ , and  $b \ll K^2$ , the parameter values used for computations are  $\lambda_w = 1.6$  cm,  $\lambda_Q = 80$  cm,  $B_w = 0.75$  T,  $B' = 5$  T/m, and  $\gamma = 400$ . From these, we have  $a_w \approx 2.8 \times 10^{-3}$ ,  $b \approx 4.75 \times 10^{-5}$ , and  $K = 0.02$ . Figures 1 and 2, respectively, show the x- and y-trajectories calculated for  $0 \leq z \leq 300/k_w$ . The initial values are chosen as  $x(0) = \bar{y}(0) = 2 \times 10^{-3}/k_w$  and  $dx/dz|_0 = dy/dz|_0 = 0$ . The analytical result here is computed from Eqs. (5)-(12). For the relatively short axial distance shown in the figures, the betatron oscillation cannot be fully displayed, but the fast oscillations induced by the wiggler can be seen clearly.

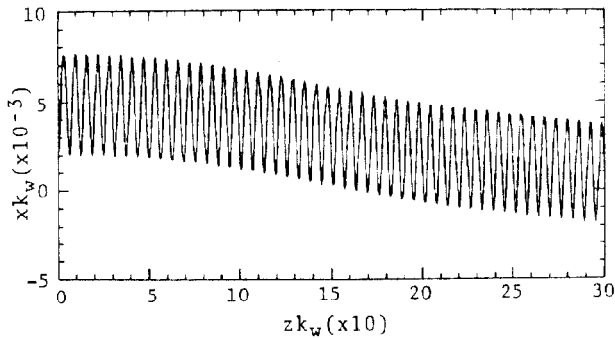


Fig. 1. Analytical and numerical results of  $x$ -trajectory for  $0 < z < 300/k_w$ ,  $a_w = 2.8 \times 10^{-3}$ ,  $b = 4.75 \times 10^{-5}$ ,  $K = 0.02$ ,  $x(0) = 2 \times 10^{-3}/k_w$ , and  $dx/dz|_0 = 0$ .

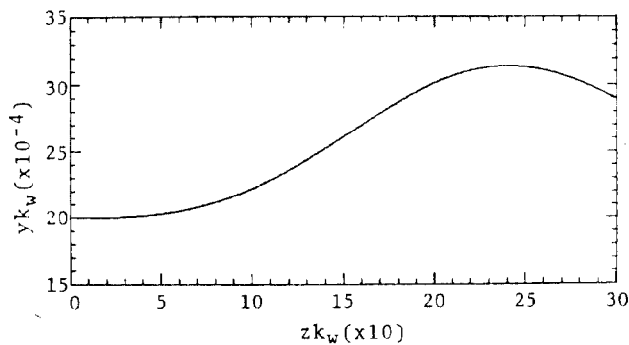


Fig. 2. Analytical and numerical results of  $y$ -trajectory for the same parameter and initial values used in Fig. 1.

In the region of  $b \ll K^2$ ,  $a_w \approx K$ , and  $K \ll 1$ , the  $x$ - and  $y$ -trajectories are shown in Figs. 3 and 4, respectively, where the analytical result of  $y$ -trajectory is calculated from Eqs. (6), (17), and (18). The parameter values and the initial conditions used are  $a_w = 0.018$ ,  $b = 4.75 \times 10^{-5}$ ,  $K = 0.02$ ,  $x(0) = y(0) = 0.002/k_w$ ,  $dx/dz|_0 = dy/dz|_0 = 0$ , and  $0 < z < 2500/k_w$ . In Fig. 3, the curve showing wiggling on the electron is densely packed in the darkened region; only the betatron oscillation and the envelope of wiggling can be recognized.

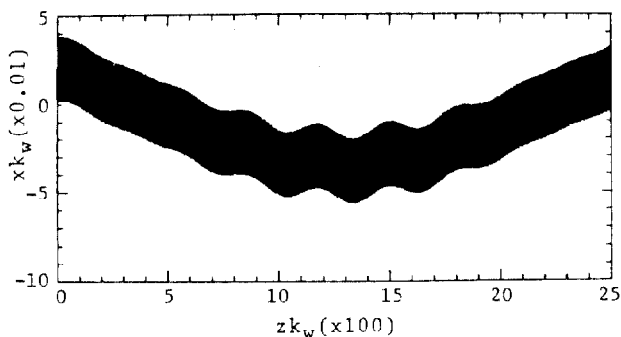


Fig. 3. Analytical and numerical results of  $x$ -trajectory for  $0 < z < 2500/k_w$ ,  $a_w = 0.018$ ,  $b = 4.75 \times 10^{-5}$ ,  $K = 0.02$ ,  $x(0) = 0.002/k_w$ , and  $dx/dz|_0 = 0$ .

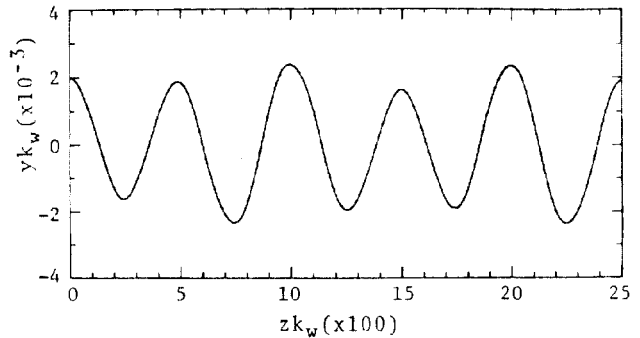


Fig. 4. Analytical and numerical results of  $y$ -trajectory for the same parameter and initial values used in Fig. 3.

### Conclusion

We have studied the electron trajectories in a combined wiggler and alternating gradient quadrupole field. Analytical solutions for the linearized equation of motion have been derived and compared with numerical solutions. The excellent agreement from the comparison suggests that the analytical results can be useful for further investigation of physical properties of an FEL with external alternating gradient quadrupole focusing such as beam envelopes, beam matching, and signal gain.

### References

1. See, for example, "Free Electron Generation of Extreme Ultraviolet Coherent Radiation," J. M. J. Madey and C. Pellegrini, Eds. (American Institute of Physics, New York, 1984), and the conference proceedings cited in the next reference.
2. B. E. Newnam, J. C. Goldstein, J. S. Fraser and R. K. Cooper, "A Linac-driven XUV Free-Electron Laser," Proc. of the Optical Society of America Topical Meeting on Free-Electron Generation of Extreme Ultraviolet Coherent Radiation, AIP Conf. Proc. No. 118 (1983), 190.
3. T. F. Wang and R. K. Cooper, "Quadrupole Focusing in Free Electron Laser (I): Beam Envelope and Matching," Los Alamos National Laboratory, Accelerator Technology Division Accelerator Theory Note, AT-6:ATN-84-15, November 1984.
4. T. F. Wang and R. K. Cooper, "Quadrupole Focusing in Free Electron Laser (II): Electron Trajectory," Los Alamos National Laboratory, Accelerator Technology Division Accelerator Theory Note, AT-6:ATN-84-16, November 1984.